

A Direct Drive System Application for Hall Effect Thrusters

IEPC-2013-278

*Presented at the 33rd International Electric Propulsion Conference,
The George Washington University • Washington, D.C. • USA
October 6 – 10, 2013*

Alessio Pampaloni¹ and Mirko Trisolini²
University of Pisa, Pisa, 56122, Italy

Tommaso Misuri³
Alta S.p.A., Ospedaletto, Pisa, 56121, Italy

and

Mariano Andrenucci⁴
Alta S.p.A., Ospedaletto, Pisa, 56121, Italy

Abstract: Hall thruster Direct- Drive system is a concrete candidate for future space missions. It is already proven that this configuration can lead to substantial benefits not only in the electric propulsion power processor but also in the thermal control system and in the Electrical Power System (EPS) system. The test target was to understand and demonstrate the Direct-Drive system operations for the Alta's low power HT-100 Hall thruster. A series of four thin-film solar panels providing up to 370 W at 270 V was directly connected to the thruster through a filter. For the purpose of this test, a LC filter was designed with a 10 μ F capacitor and a 1 mH inductor. Thruster operations resulted correct and stable. The system performance throttling was carried out via anode flow rate regulation and this method came out to be simple and effective. Two ignition procedures, soft start and hard start, were investigated by taking the current data during startup transient. The hard start proved to be more demanding but in both cases the thruster ignited properly. Filter performance were also evaluated by comparing the RMS value of the measured current oscillations on thruster side and solar array side during steady state operations. The data evidences that the filter is always capable to dampen thruster current peaks; the RMS on the solar array side remained almost constant in all the tested operative conditions.

Nomenclature

| | |
|-----------|--|
| f_I | = current mismatch coefficient |
| f_V | = voltage mismatch coefficient |
| G | = solar irradiance, W/m ² |
| G_0 | = baseline solar irradiance for panel performance data, W/m ² |
| I_{AVG} | = average value of the current, A |
| I_{pp0} | = panel current at peak power point, at standard conditions, A |
| I_{pp} | = panel current at peak power point, A |
| I_{RMS} | = RMS value of the current, A |
| I_{sc0} | = panel short-circuit current at standard conditions, A |

¹ Graduate Student, Department of Civil and Industrial Engineering, University of Pisa

² Graduate Student, Department of Civil and Industrial Engineering, University of Pisa

³ Project Manager, Coordinator of Electric Propulsion Activities, Alta S.p.A.

⁴ President, Alta SpA; Professor of Electric Propulsion and Space Systems, University of Pisa

| | |
|------------------|---|
| I_{sc} | = panel short-circuit current, A |
| N | = number of samples |
| T_0 | = baseline cell temperature for panel performance data, °C |
| T_C | = cell operating temperature, °C |
| V_{oc0} | = panel open-circuit current at standard conditions, V |
| V_{oc} | = panel open-circuit current, V |
| V_{pp0} | = panel voltage at peak power point, at standard conditions, V |
| V_{pp} | = panel voltage at peak power point, V |
| $\beta_{I_{pp}}$ | = temperature coefficient for panel peak-power current, 1/°C |
| $\beta_{I_{sc}}$ | = temperature coefficient for panel short-circuit current, 1/°C |
| $\beta_{V_{oc}}$ | = temperature coefficient for panel open-circuit voltage, 1/°C |
| $\beta_{V_{pp}}$ | = temperature coefficient for panel peak-power voltage, 1/°C |

I. Introduction

The attractiveness of the electric propulsion and its effective use in space missions are becoming more and more widespread in the last two decades. Hence, the interest in simplifying the power processor dedicated to the electric propulsion system is a natural consequence. The Direct-Drive well fits into this context since it allows the anode supply removal which is the most impactful element of the Power Processing Unit (PPU) in terms of mass, complexity and thermal burden. Therefore, the Direct-Drive implementation would lead to direct advantages which involve the thermal control system and the electric propulsion system. Important mass savings can be also exploited in an indirect way. The fact that the solar array must provide power to the thruster at high voltage (about 300 V) gives the opportunity to design a high voltage bus. Even if the high voltage solar array and the high voltage bus entail technological issues, the latter configuration improves the electric power system efficiency and thus reduces its mass. Of course the type of mission has to be considered (orbit, payload, duration, etc.), but it has been already demonstrated that the high voltage bus arrangement could lead to substantial mass benefits (e.g. GEO).^{1,2}

Although the Direct-Drive concept was born in the seventies in relation with the NASA's 30-cm-diameter, mercury fueled, gridded-ion thruster, it is only in the last two decades, in parallel to the Hall thruster advent in the western market, that it has become a real candidate for future missions. The first experimental test with a Hall thruster was carried in 1995 by Hamley et al. where the 4.5 kW T-160 was supplied by a 1 kW solar array.³ Then, Brandhorst et al. successfully ignited and operated the 1.3 kW T-100 Hall thruster from a triple junction linear concentrator solar array.⁴ A very important evidence of the current interest in the Direct-Drive system was the NASA decision, in 2011, to install the National Direct-Drive Testbed, a 12 kW solar array system characterized by terrestrial silicon solar cells. This high-power facility, in addition to supplying for the first time a high-power Hall thruster, allows investigating all the Direct-Drive related issues appeared in previous tests. The experimental investigation of Snyder et al. is the most detailed and extensive campaign to date; they studied the Direct-Drive system performance of the 6kW H6 Hall thruster.⁵

The present work takes the cue from this experimental investigation to carry out the first European Direct-Drive system demonstration implemented in the Alta's HT-100 low power thruster.

II. Test Setup

A. Hall Thruster

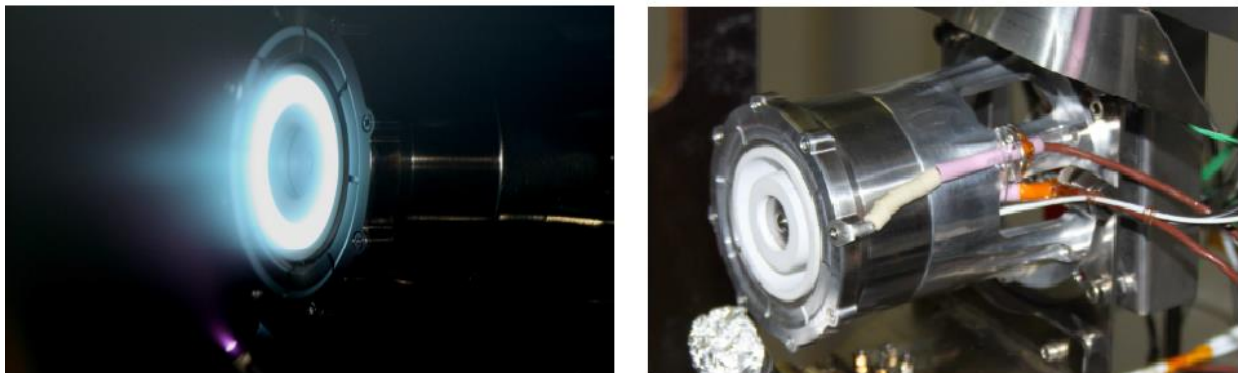


Figure 1. HT-100 firing at Alta IV-4 test facility (left) and HT-100 mounted on ALTA thrust balance (right)

The HT-100 (Fig. 1) Hall Thruster⁶ was selected for the Direct-Drive demonstration. The thruster, fully developed by Alta, is a low power device designed for orbit and attitude control of small spacecraft with low power production capability. The throttling range of the thruster is approximately 100-300 W discharge power, 800-1200 s specific impulse, 5-12 mN thrust, with an efficiency up to 35%. The discharge voltage ranges from 150 V to 400 V whereas the discharge current varies between 0.15 A and 1.5 A. The magnetic field is generated by permanent magnets. The EM (Engineering Model) thruster is equipped with a discharge chamber made of a mixture of BN/SiO₂ (60/40), a conventional anode and propellant distribution. The thermal load is dissipated by the outer case radiating surface and the thruster body is insulated from the thrust stand by means of a cylindrical hollow mounting interface.

The HT-100 hollow cathode design has been recently improved and the Direct Drive test was carried out in the early phase of a new cathode life during which its performance had not yet reached the desired one. This means that during tests the matching between the thruster and the cathode was not optimized. Although it is designed to work only during startup, for correct thruster operations the cathode keeper was required to be always active, also after the ignition phase.

B. Solar Array

The solar array configuration consists of a set of four terrestrial solar panels populated by thin film amorphous silicon solar cells. Each panel is 1.30 m × 1.10 m and is capable to provide 90 W at peak power point in standard atmospheric conditions (1000 W/m², AM 1.5 and 25 °C) with an efficiency of 6.3%.⁷ The short circuit current and the open circuit voltage of a module are respectively 1.56 A and 95.3 V in standard atmospheric conditions. The four modules were connected in series in order to reach a nominal open circuit voltage of 381.2 V. After the installation of the solar array, measurements revealed that the performance were different from the nominal ones. This was not totally unexpected as the manufacturer states that the solar modules can show better performance during the first six weeks of operation.

The solar array was placed near Alta's IV-4 vacuum chamber facility and arranged in a south-facing structure tilted of an angle of 35°. The tilt angle was selected using a solar irradiance prediction code based on the Bird model⁸, in order to achieve maximum irradiance during the test timespan.

The solar panel configuration was chosen in order to match the HT-100 voltage and current characteristic: the goal was to obtain an I-V curve that allowed to test the Direct Drive system at the solar panel peak power point. In this context the choice of the thin film solar cells technology was made since it is suitable to provide power at high voltage and low current which are basic requirements for HT-100 proper operation.



Figure 2. Direct-Drive solar array arrangement

In addition, an electrical box has been installed to ensure safe operation and manage the switching of the system. The box includes a 1000 Vdc breaking and manoeuvring switch and a couple of 2 A fuses.

C. Test Facility and Instrumentation

The thruster was tested in the Alta's IV4 facility⁹ which represents the cornerstone of Alta's Hall thruster test activities. This chamber consists of a main vessel (Auxiliary Chamber), 2 m in diameter and 2.5 in length, connected through a 1 m gate valve to a service chamber (Small Chamber), 1 m in diameter and 1 m in length. The facility is equipped with two independent oil-free pumping system, one connected to the main vessel and the other connected to the service chamber for redundancy. The pumping system is constituted by a 25 mc/hr rotary pump, a 2000 l/s turbomolecular pump used for evacuation, a cryogenic high vacuum stage based on 1 x 3000 l/s cryopump and a 6 x 12000 l/s custom cold plates. The pumping speed reached is about 70000 l/s allowing for an ultimate vacuum level lower than 10⁻⁷ mbar. In order to reduce the contamination of the thruster due to the back-sputtering from the facility walls during long duration tests, a bi-conical beam target lined with high purity graphite has been designed and accommodated in front of the thruster inside the opening cap of the facility.

Xenon flow was regulated with standard laboratory system and the cathode ignition and operation were controlled with a dedicated power supply.

The current oscillations were recorded using a digital oscilloscope both during steady state operation and start up transient. Measurements of oscillations were performed using a clamp-on current probe. Acquisition of data was performed collecting 1×10^6 points with a sample interval of $1 \mu\text{s}$.

Global solar irradiance were measured using a pyranometer located near the solar array. In order to obtain values of irradiance incident on the solar array the pyranometer was inclined of 35° , the same inclination of the solar panels.

The temperature of the solar cells was measured with a thermocouple positioned on the backside of the solar panels, assuming that the cell temperature is the same of the coverglass of the panel.

III. Test Background

A. Solar Array Performance Model

In a Direct-Drive system there is a strong correlation between thruster performance and solar array characteristic. For this reason it is important to understand which are the factors affecting the solar array I-V curve and how they influence it.

The solar array performances are mainly affected by two parameters: the irradiance and the cell temperature. A peculiarity of the amorphous silicon thin film cells is that the temperature impact on their performance is less significant with respect to the common silicon cells. Manufacturer provides the temperature coefficients which take into account the temperature effect on solar array voltage and current.⁷ Then, the losses (in the wires, connections and the ones due to cells mismatching factors) can be estimated during the photovoltaic system operations and their effect, in order to obtain a realistic I-V curve, must be included in the equations.

In this work, the curve has been plotted from the knowledge of the values of the short circuit current (I_{sc}), the voltage (V_{pp}) and current (I_{pp}) at the peak power point and the open circuit voltage (V_{oc}). The equations relating these quantities to the irradiance (G), cells temperature (T_c) and losses are the following:¹⁰

$$I_{sc} = I_{sc0} \frac{G}{G_0} f_I [1 + \beta_{Isc} (T_c - T_0)] \quad (1)$$

$$I_{pp} = I_{pp0} \frac{G}{G_0} f_I [1 + \beta_{Ipp} (T_c - T_0)] \quad (2)$$

$$V_{pp} = V_{pp0} \frac{G}{G_0} f_V [1 + \beta_{Vpp} (T_c - T_0)] \quad (3)$$

$$V_{oc} = V_{oc0} \frac{G}{G_0} f_V [1 + \beta_{Voc} (T_c - T_0)] \quad (4)$$

Where the subscript 0 refers to standard conditions and f_I and f_V are the mismatch coefficients.

Once the four values (I_{sc} , V_{pp} , I_{pp} , V_{oc}) are derived from the equations, a simple curve fitting can be performed in order to obtain the solar array I-V curve. Furthermore, also the power-voltage curve can be plotted considering that the power is simply the voltage times the current.

The losses in the solar array power system were estimated by measuring its real performance. The voltage loss in the wires and connections from the arrays to the thruster was measured and resulted to be 4 V (this value was taken as constant). After the analysis of several data, the mismatch coefficients (f_I , f_V) were set to 1. Although the assumption for the voltage coefficient is very common, the one involving the current coefficient may seem unrealistic. However this decision is coherent with the measured over-performance of the solar array previously anticipated (paragraph II B). Analyzing the data of the measurements, while the open circuit voltage of the solar array was practically the nominal one (380 V) the short circuit current in standard condition was found to be 1.69 A which is about the 8% higher than the nominal value (1.56 A). This circumstance confirms that these modules perform better in their early life.

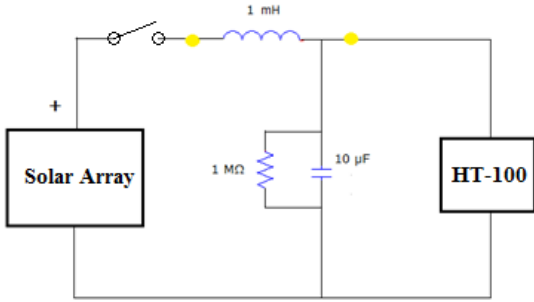


Figure 3. Direct-Drive electrical schematic

capacitor in parallel and a 1 mH inductor in series (Fig.3). Also a 1 MΩ bleed resistor was placed in parallel to the capacitor in order to discharge the capacitor after thruster shut-down. Despite the filter's performance revealed to be completely satisfactory a further optimization of the filter could be carried out.

In Fig.3 the switch of the electrical box is also shown together with the locations of the current probe during current oscillations measurements (yellow points).

B. Experiment Electrical Layout

The electrical schematic for a Direct-Drive system is shown in Fig. 3. The solar array output is directly connected to the thruster with an interposed filter.

The filter is an essential element of a Direct-Drive system since it has the function of damping the thruster oscillations in order to ensure the correct functionality of the solar array. Alta's laboratory power supply is not equipped with a filter unit since it is oversized for the HT-100 requirements. Therefore one of the first steps in the Direct-Drive implementation was the design of a proper filter. The selected configuration was characterized by a 10 μF electrolytic

IV. Experimental Results

A. Direct-Drive system regulation

The first attempt to turn on the thruster in a Direct Drive mode was performed with the following procedure: the open circuit voltage was applied between anode and cathode and then the propellant flow rate was gradually increased until the thruster ignited at a value of 0.5 mg/s. In this operating condition the anode current was 0.45 A and the anode voltage was 333 V. The ignition occurred at the first attempt with no issues observed; the operation was stable for several minutes. The cathode, always operative during the whole test, was set to a flow rate of 1 mg/s corresponding to a current of 1.5 A; these values were maintained constant for the full duration of the test.

Then, the operating conditions were changed by stepwise increment of the anode flow rate. The figure 4 shows the sequence of the operating conditions and the trend of the irradiance during the whole test timespan (Italian summer time).

After the proved stability of operations the xenon flow rate was increased to 0.6 mg/s corresponding to a discharge voltage of 330 V and an anode current of 0.50 A. Then, after few minutes the flow rate was again increased at 0.7 mg/s, 1 mg/s, 1.25 mg/s and 1.5 mg/s whose corresponding values of current and voltage are shown in table 1. In particular, at 1.5 mg/s the solar array peak power point was reached with a current of 1.37 A, a voltage of 269 V and thus a discharge power of 368 W. Since the HT-100

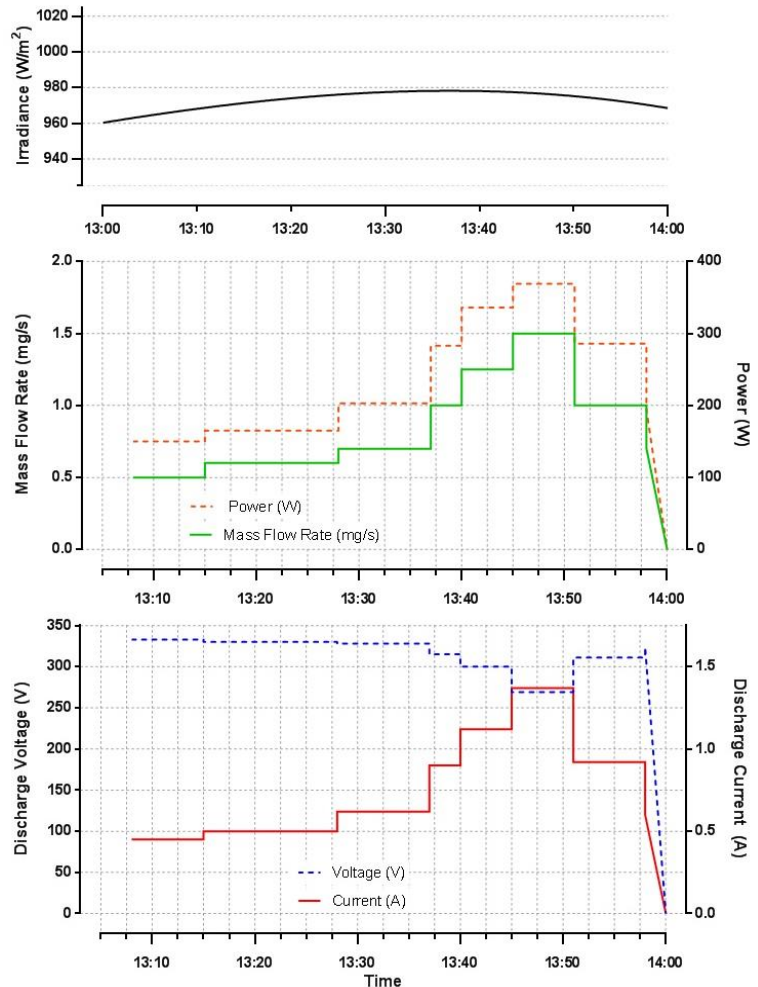


Figure 4. Test sequence of the HT-100 Direct-Drive operations

was not designed to operate at such high values of power and anode current, the propellant flow rate was not increased any further and this operative condition was maintained just for a few minutes. At this point, the flow rate was decreased, first at 1 mg/s, and then gradually up to the extinction of the discharge which occurred at 0.7 mg/s.

Thrust measurements were performed at the ignition (8 mN) and at the peak power point condition (17 mN). The latter value is consistent with the thrust expected for HT-100 operation at high power levels (here exceeding 300W).

The system performance control via stepwise xenon flow rate regulation came out to be a simple and reliable method for thruster throttling. The HT-100 responded correctly and quickly to the imposed variations of the operative conditions, even when the mass flow rate change was significant (e.g. from 0.7 mg/s to 1 mg/s and from 1.5 mg/s to 1 mg/s).

The thruster started up at the first attempt; we expected that the ignition would have occurred at a higher value of mass flow rate since the HT-100 usually ignites at least at 0.7 mg/s when connected to the laboratory power supply. Instead, in this case, a value of 0.5 mg/s was enough to trigger the discharge.

In the Fig. 5-6 the tested operating conditions are depicted on the solar array I-V and P-V curves. The test was carried out during solar noon; in the whole test timespan, the irradiance and cells temperature variation was small and thus the solar panel output performance remained almost constant. In fact, the irradiance varied between 967 and 979 W/m² whereas the cell temperature ranged from 50 °C to 51 °C.

Summarizing, no issues were observed and the thruster correctly operated from the ignition to the extinction of the discharge, reaching a level of power well beyond its standard value.

B. Thruster ignition

The system performance investigation at ignition was studied with two different procedures: the soft start and the hard start. This kind of distinction had been suggested by Snyder et al.⁵ In the first procedure the open circuit array voltage is applied between the anode and the cathode and then a mass flow rate is gradually incremented until the discharge ignites. On the other hand, the hard start is carried out by first establishing the mass flow rate at the desired value and then, using a switch, the array power is instantaneously delivered to the thruster. This distinction between the two procedures is characterized by the magnitude of the current overshoot; in fact during the hard start the current peak is more demanding.

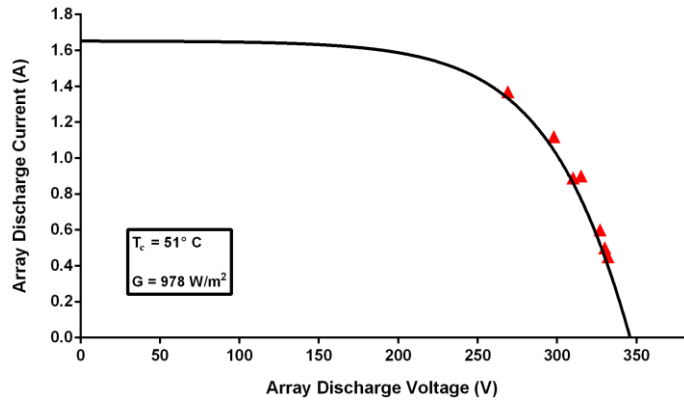


Figure 5. Current-Voltage curve during test runtime and thruster operative condition

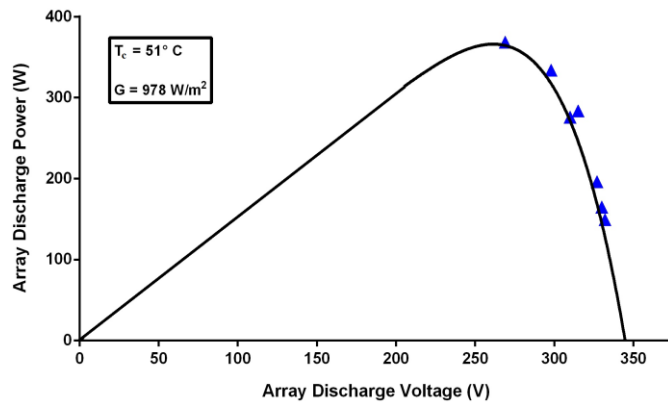


Figure 6. Power-Voltage curve during test runtime and thruster operative condition

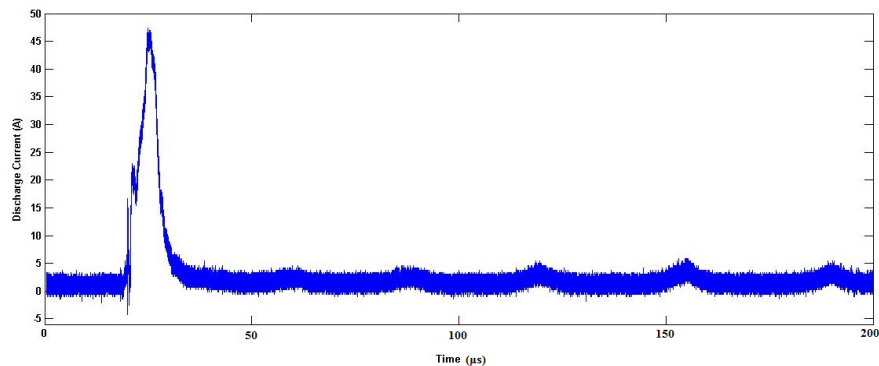


Figure 7. Ignition transient during Soft Start on thruster side

Both for the soft start and the hard start procedure measurements of current waves were taken before and after the filter. First, the soft start was investigated at a propellant flow rate of 1.25 mg/s. Fig. 7 and 8 show respectively the current wave on the thruster side and on the solar array side. It is possible to notice that the current peak required by the thruster is about 45 A whereas the solar panels “see” only 4.5 A, the charge difference being in fact provided by the filter. It is possible to notice that, in this case, the mass flow rate necessary for the thruster ignition was higher than the one used in the previous part of the test. This was probably due to anode overheating after several minutes of operation at a power level in excess of 300W (accumulated in the previous phase of the test).

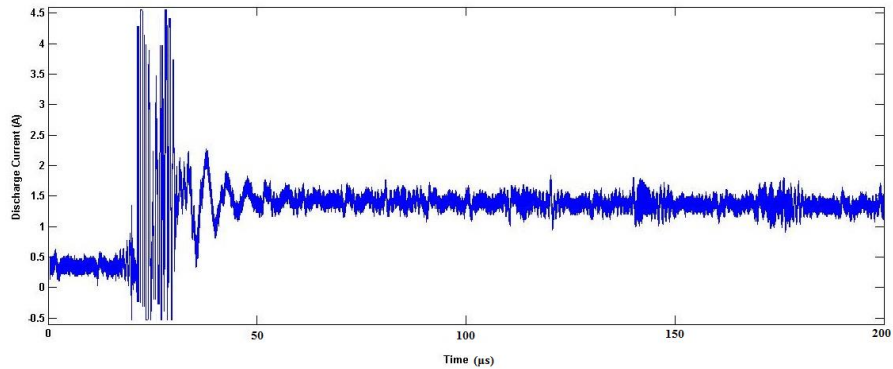


Figure 8. Ignition transient during Soft Start on solar array side

Then, the hard start was tested: while the thruster chamber was filled by 1.25 mg/s of gas propellant the switch of the electrical box was closed and the thruster started. Fig. 9 and 10 show the current wave for the hard start case on both the thruster and panel side. In this situation the thruster current peak reached almost 80 A whereas the arrays current was 18 A. These values are significantly higher than the ones measured for the soft start, confirming that hard start is the most demanding ignition procedure.

The Fig. 7-10 show that the filter was very effective in “shielding” the solar array from the high current peaks produced by the HT-100 Hall thruster during ignition, both during the soft start and the hard start procedure. In fact in the former case (soft start) the current peak on the panel side was more than ten times smaller than the one experienced on the thruster side; in the latter case (hard start) the current peak was reduced by more than four times.

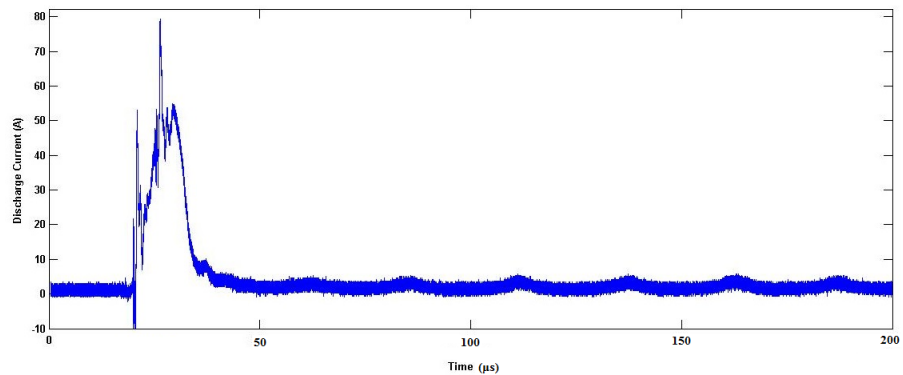


Figure 9. Ignition transient during Hard Start on thruster side

A curious behavior of the array power system is that, during start up transient, it delivers a current peak well beyond its nominal possibilities; for instance, during the hard start transient, the array current overshoot is about 18 A that is, by far, greater than the value of the short circuit current (1.69 A). This circumstance was already observed in similar tests⁵ and it is thought that it is due to the stray capacitance of the solar array system. At the start up, when a large amount of charge is required by the thruster, the filter capacitor takes care of providing this current but also the solar array ‘helps’ the system by

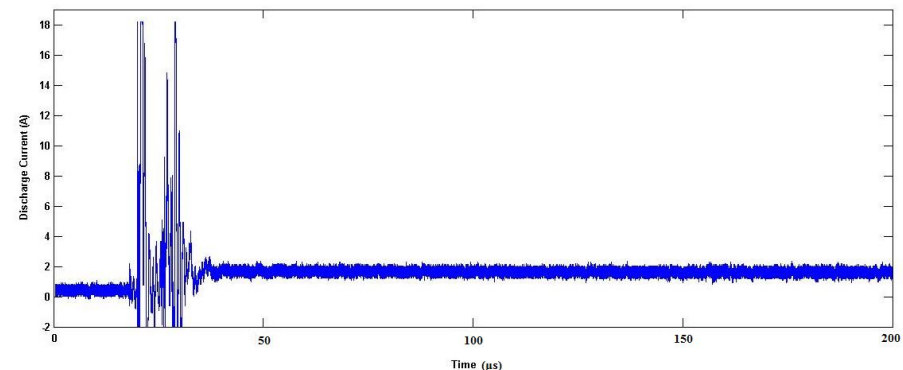


Figure 10. Ignition transient during Hard Start on solar array side

delivering charge to the capacitor and the thruster. This is not a nominal operation of the array system (in fact it is not describable in terms of I-V curve) and it can be explained by the unexpected presence of capacitive effects in its structure, connections, cells, etc.

C. Thruster Oscillations

In this paragraph the filter performance during thruster steady state operation are presented. The HT-100 exhibits breathing oscillations in the range of 30-40 kHz depending on the operating condition. As already stated, the main task of the filter is to dampen these oscillations in order to allow a safe and stable system operation. The results of the test are shown in Fig. 11 where the RMS values of the current oscillations are given for both the thruster side and the panel side. It is important to outline that the RMS data presented here were determined removing the DC component of the current signal (I):

$$I_{RMS} = \sqrt{\frac{\sum (I - I_{AVG})^2}{N}} \quad (5)$$

Where N is the number of samples.

As a first result, it can be seen that the solar array current RMS is always attenuated by the filter and it means that it effectively worked in all the tested operative conditions.

The oscillations on the thruster side were almost constant except at low mass flow rates (less than 0.7 mg/s) where the fluctuations are visibly lower. These conditions are not standard for the HT-100, in fact it is usually ignited at higher values of propellant flow rate and it generally does not sustain the discharge in this condition; indeed in this test the discharge extinguished at 0.7 mg/s. On the solar array side, the RMS value of the current was almost constant in all the operative conditions.

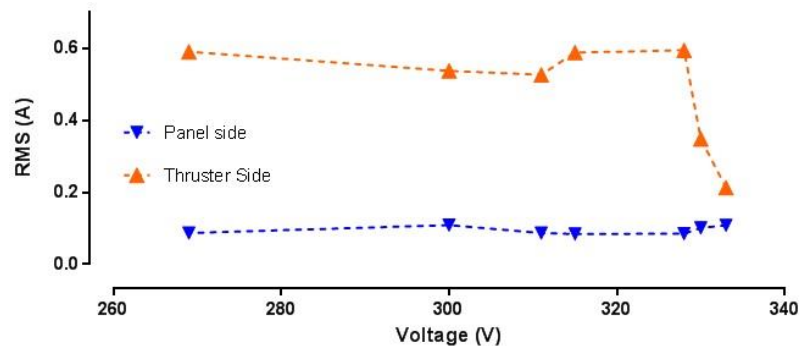


Figure 11. RMS value of current oscillations on thruster side and solar array side

V. Conclusion

A Direct-Drive system demonstration was successfully carried out at ALTA's laboratories. The Hall thruster HT-100 correctly started up and operated at a discharge power ranging from 150 W to 370 W. No anomalous behavior was detected and the test completely proved that direct connection to solar arrays can be a concrete candidate solution for electric thruster supply.

The system performance regulation was carried out by means of anode propellant flow rate variation which came out to be a simple and reliable method for control of thruster operating conditions.

Two modes of ignition were tested: a soft start and a hard start. Both the procedures ensured a correct discharge start, even if the first one involves lower current peak and thus a smaller stress for the electrical circuit. The soft start occurred at a flow rate of 0.5 mg/s which is a very low value for the standard HT-100 operations.

A dedicated LC filter was designed from scratch and employed during the Direct-Drive test. Starting from circuit simulations with Pspice and continuing with experimental tests with the laboratory power supply, the filter arrangement was fixed with a 10μF capacitor and a 1 mH choke. It ensured thruster-solar panel compatibility and provided satisfactory results in terms of current oscillations damping both during start-up and steady state operations. Further tests can be setup in order to optimize its configuration.

The solar panel worked with no issues in all the tested conditions, from the ignition (333 V, 0.45 A) to the peak power (269 V, 1.37 A). A singular event occurred at the start-up, in fact during this transient the solar array provided a current overshoot (up to 18 A) well beyond its nominal possibility (1.67 A). This event is probably caused by the stray capacitance of the solar array.

During the planning of the experiment, an effort was made in understanding which were and how several factors affect photovoltaic system performance since this is strictly related to thruster operations in a Direct Drive system.

In this direction, a solar irradiance prediction model was studied and, complementarily, a model relating the environmental factors and the solar panel I-V curve was employed. Incidentally, this part of the work allowed to realize a 35° inclined ancillary structure capable to optimize the irradiance incident on the cells surface.

References

¹Hoskins, W. A., Homiak, D., Cassady, R. J., Kerslake, T., Peterson, T., Ferguon, D., Snyder, D., Mikellides, I., Jongeward, G. and Schneider, T., "Direct Drive Hall Thruster System Development," AIAA-2003-4726, 39TH AIAA/ASME/SAE/ASEE Joint Propulsion Conference and Exhibit, Huntsville, Alabama, July 20-23, 2003.

²Brophy, J. R., Gershman, R., Strange, N., Landau, D., Merrill, R. G., and Kerslake, T., "300-kW Solar Electric Propulsion System Configuration for Human Exploration of Near-Earth Asteroids," AIAA 2011-5514, 47th Joint Propulsion Conference, San Diego, California, July 31 – August 3, 2011.

³Hamley, J. A., Sankovic J. M., Miller J. R., O'Neill M. J., Lynn P., Oleson S. R., "Hall Thruster Direct Drive Demonstration," 33rd Joint Propulsion Conference, Seattle, WA, July 6-9, 1997.

⁴Brandhorst, Jr., H.W., Best, S.R., Rodiek, J.A., O'Neill, M.J., and M.F. Piszczor, Jr., "Direct-Drive Performance of a T-100 HET Powered by Triple Junction, High-Voltage Concentrator PV Array", AIAA 2010-6620, 46th Joint Propulsion Conference, Nashville, TN, July 25-28, 2010.

⁵Snyder J. S., Brophy J. R., Hofer R. R., Goebel D. M., and Katz I., "Experimental Investigation of a Direct-Drive Hall Thruster and Solar Array System at Power Level up to 10 kW", AIAA 2012-4068, 48th AIAA/ASME/SAE/ASEE Joint Propulsion Conference & Exhibit, Atlanta, GA, 30 July - 01 August, 2012

⁶Dignani, D., Ducci, C., Cifali, G., Rossetti, P., Andrenucci, M., "HT-100 Hall Thruster Characterization Results," 32nd International Electric Propulsion Conference, Wiesbaden, Germany, September 11-15, 2011. *Periodicals*

⁷*MPE-90-AL-01 Datasheet*, Schüco, Available from: http://www.schueco.com/web/de-en/architekten/solarstrom_und_waerme/produkte/solarpower/schueco_dunnschichtmodule_MPE_AL_serie [Cited April, 2013].

⁸Bird, R.E. and R.L. Hulstrom, *A Simplified Clear Sky Model for Direct and Diffuse Insolation on Horizontal Surfaces*, SERI report TR-642-761, Solar Energy Research Institute, Golden, CO, Feb. 1981.

⁹*IV-4 Vacuum Facility Datasheet*, Alta SpA, Available from: <http://www.alta-space.com/uploads/file/brochures/IV4%20Vacuum%20Facility.pdf> [Cited April, 2013]

¹⁰Rauschenbach, H.S., *Solar Cell Array Design Handbook*. 1976, New York: Van Nostrand Reinhold.